Field demonstration of simultaneous wind and temperature measurements from 5 to 50 km with a Na double-edge magneto-optic filter in a multi-frequency Doppler lidar

Wentao Huang,[1] Xinzhao Chu,[1,*] Johannes Wiig,[1] Bo Tan,[1] Chihoko Yamashita,[1] T. Yuan,[2] J. Yue,[2] S. D. Harrell,[2] C.-Y. She,[2] B. P. Williams,[3] J. S. Friedman,[4] and R. M. Hardesty[5]

[1]*University of Colorado at Boulder, 216 UCB, CIRES, Boulder, Colorado 80309, USA*
[2]*Colorado State University, Fort Collins, Colorado 80523, USA*
[3]*Northwest Research Associates Colorado Research Associates, 3380 Mitchell Lane, Boulder, Colorado 80301, USA*
[4]*National Astronomy and Ionosphere Center Arecibo Observatory, HC-03 Box 53995, Arecibo, Puerto Rico 00612*
[5]*National Oceanic and Atmospheric Administration Earth System Research Laboratory, Boulder, Colorado 80305, USA*
**Corresponding author: Xinzhao.Chu@Colorado.edu*

Received February 10, 2009; revised April 12, 2009; accepted April 13, 2009; posted April 15, 2009 (Doc. ID 107400); published May 12, 2009

We report the first (to our knowledge) field demonstration of simultaneous wind and temperature measurements with a Na double-edge magneto-optic filter implemented in the receiver of a three-frequency Na Doppler lidar. Reliable winds and temperatures were obtained in the altitude range of 10–45 km with 1 km resolution and 60 min integration under the conditions of 0.4 W lidar power and 75 cm telescope aperture. This edge filter with a multi-frequency lidar concept can be applied to other direct-detection Doppler lidars for profiling both wind and temperature simultaneously from the lower to the upper atmosphere. © 2009 Optical Society of America

OCIS codes: 280.3640, 010.3640, 290.1310, 010.3920, 120.0280, 300.6210.

Simultaneous profiling of wind and temperature from the lower to the upper atmosphere is a capability urgently needed for whole-atmosphere research and wave-coupling studies from the wave source region in the lower atmosphere to the wave impact region in the middle and upper atmospheres. Doppler lidars based on Fabry–Perot interferometers and iodine filters have achieved wind [1–3] or temperature [4] measurements but not both, unless a temperature channel is added to the wind lidar. This is because only one frequency is used in the lidar transmitter, leading to a single ratio for either wind or temperature derivation. In an earlier publication [5], we proposed to incorporate a Na double-edge magneto-optic filter (Na-DEMOF) into the receiver of a three-frequency Na Doppler lidar. The three frequencies of the lidar would result in three independent ratios, enabling simultaneous wind and temperature measurements from the troposphere to the stratosphere [5]. Combined with the Na Doppler lidar measurements in the mesosphere and lower thermosphere (MLT) [6], it is possible to profile both wind and temperature from the lower to the upper atmosphere. In this Letter, we implement the hot-cell Na-DEMOF that we developed and characterized in [5] into the receiver of the Colorado State University (CSU) Na Doppler lidar. The initial sky tests demonstrate the wind and temperature profiling from 5 to 50 km with this multi-frequency edge-filter technique.

Illustrated in Fig. 1 is the experimental setup used in the first sky test on 16 October 2008 at Fort Collins, Colorado (40.6°N, 105°W). The CSU Na Doppler lidar is a dye-ring-laser-based system [6] that operates at three frequencies sequentially: $f_a = -651.4$ MHz and $f_{\pm} = f_a \pm 630$ MHz relative to the Na D_2 line center near 589 nm. The laser beam (~20 mJ per pulse at 50 Hz) is split and then transmitted to the atmosphere in three directions for vector wind measurements. Three telescopes are pointed to these three directions to collect backscattered photons. The east-pointing telescope (20° off-zenith) with a diameter of 75 cm was chosen as our test channel (~17% laser power). The light collected by the telescope is coupled to a multimode fiber with a 1.5 mm core that directs the light to the Na-DEMOF receiver chain. As described in [5], the Na cell in medium magnetic field acts as a double-edge filter, so different absorptions are experienced by the left- and right-circular polarization components of the light that passes through the polarizer (P1). Exiting the cell, the intensity ratio of these two components is a sensitive function of

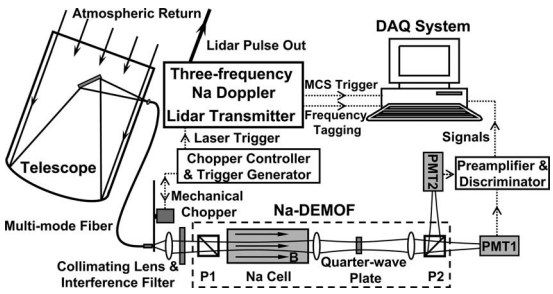

Fig. 1. Experimental setup for the field tests of a hot-cell Na-DEMOF with the three-frequency Na Doppler lidar. The Na cell temperature is stabilized within ±0.1°C at 160°C, and the magnetic field is 1350 Gauss.

Doppler wind and temperature [5]. To measure this ratio, these two components are converted to two crossed linear polarizations by the follow-up quarter-wave plate and then separated by the polarized beam splitter (P2) to two photomultiplier tubes (PMTs) running in photon-counting mode. The PMT signals are discriminated and fed to the computer multichannel scaler card for data acquisition (DAQ). The bin width was set to 0.5 μs, corresponding to a range resolution of 75 m. Typical lidar raw data for this test are shown in Fig. 2(a). Since the lidar returns at each of the three frequencies are split into two channels corresponding to the left- and right-circular polarizations, we ultimately obtain six channels of signals. The relative strengths of these signals resemble what we expected from the simulation in [5]. In general, we have photon counts $N_{R-}>N_{Ra}>N_{R+}>N_{L+}>N_{La}>N_{L-}$ around 220 K and 0 m/s, where L and R represent the left and right channels, while $+$, $-$, and a denote the lidar operating frequencies of f_+, f_-, and f_a. The decrease of signals below 3 km is due to the reduced overlap between the receiver field of view and the lidar beam divergence.

The data-processing procedure for deriving wind and temperature is not as straightforward as single-frequency direct-detection Doppler lidars, but rather close to the ratio techniques applied in the Na Doppler lidars [6]. Using the metrics R_W and R_T proposed as Eq. (1) in [5], we compute two ratios from the preprocessed lidar data: R_W from f_+ and R_T from f_- frequencies. On the two-dimensional theoretical calibration curves given as Fig. 3 in [5] we draw two straight lines at the two ratios on the horizontal and vertical axes, respectively. The cross point of these two lines gives a point on the calibration curves, from which we infer the line of sight (LOS) wind and temperature that generate these two ratios. This lookup table procedure is done for each altitude, and thus we obtain the range-resolved profiles of LOS wind and temperature. Two major issues in the data processing are the signal-to-noise ratio (SNR) and the system calibration. In preprocessing, the raw data are sorted by frequencies and channels and then integrated to yield 1 km and 30 min resolutions to improve the SNR. The photon returns from 130 to 140 km are used to estimate and subtract the background counts from the integrated profiles. The theoretical calibration curves are calculated under ideal conditions, e.g., the identical optical efficiency for the left and right channels, the linear response of PMTs to any count rate, and aerosol-free conditions; however, the actual situation deviates from these ideals. Thus, careful calibration is needed in order to derive the two ratios R_W and R_T properly. We introduce two types of calibration factors in our analysis: the factor A to account for the different optical efficiencies in the two detection channels, and the B factors to account for PMT nonlinearity for different channels with different count rates. We manually rotate the quarter-wave plate by 90° to compare the photon counts of the same signal detected by the two different channels; thus the calibration factor A is found to be 4.07. As for the B factors, they should be, in principle, derived from an independent PMT calibration. Lack of a calibrated light source prevents us from doing so. For this demonstration, we calibrate the measurements to the radiosonde data at Denver (39.8°N, 104.9°W), 88 km distant from CSU, by introducing two altitude-independent scaling numbers: one for N_{R+} and another for N_{R-}. Through minimizing the standard deviations between the lidar and radiosonde data in the altitude range of 8–12 km, these two numbers are determined to be 1 and 1.15, respectively. The retrieved LOS wind and temperature for this first field test are plotted in Fig. 3. The low quantum efficiency (QE, ~2% at 589 nm) of the two PMTs (EMI 9214B) is the main cause for the measurements being limited to ~16 km.

To extend the measurement range, we used a PMT (Hamamatsu H7422) with high QE (~40%) and split more laser power (~0.4 W) to boost up the signal levels in the followup field tests on 11 December 2008

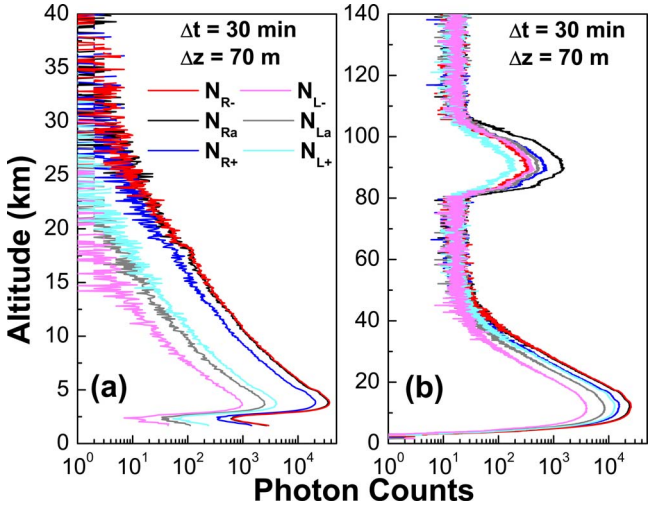

Fig. 2. (Color online) Raw lidar data profiles obtained on (a) 16 October 2008 with two PMTs and (b) 11 December 2008 with one PMT. Vertical resolution is $\Delta z = 75 \times \cos(20°) = 70$ m.

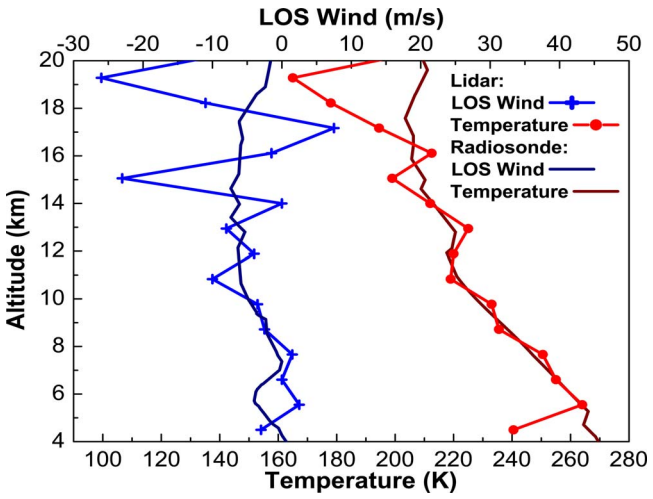

Fig. 3. (Color online) Retrieved LOS wind and temperature on 16 October 2008. The integration time Δt is 30 min, and the vertical resolution Δz is 1 km. The wind and temperature errors are about ±1.1 m/s and ±2.2 K at 9.8 km.

and 9 January 2009. Unfortunately, only one high-QE PMT was available at the time, so we had to switch between polarizations every 5 min by rotating the quarter-wave plate 90° inside the Na-DEMOF. This allowed PMT1 to detect the two polarizations sequentially. A chopper was used to block the strong low-atmosphere returns to protect the PMT. The obtained raw data in Fig. 2(b) are nearly 100 times stronger than the first test, and the Na fluorescence is visible from 80 to 105 km. In the data processing the calibration factor A is not needed for this setup, since the same optical path and PMT were used. But half of the integration time is lost when switching between the two polarizations. The altitude-independent scaling numbers are determined to be 1.19 and 2.85 by minimizing the standard deviations from 25 to 30 km. The derived LOS wind and temperature are successfully extended to nearly 50 km [Fig. 4]. Between 10 and 30 km, both the retrieved wind and temperature match the radiosonde data well, considering these observations are 88 km and a few hours apart; from 10 to 45 km, they are close to the model data of the Mass Spectrometer Incoherent Scatter (MSIS) and the United Kingdom Met Office (UKMO). This is true for both field tests with the high-QE PMT. Wavy structures observed in the wind and temperature below 40 km are likely caused by dynamic activity in the atmosphere; however, the large shears above 40 km are likely due to photon noise. The lower limits of measurement uncertainties calculated using Eq. (2) given in [5] are shown as ΔV_{LOS} and ΔT in Fig. 4.

These field tests are the first (to our knowledge) proof of concept for this Na-DEMOF-based multi-frequency Doppler lidar to measure wind and temperature simultaneously from 10 to 45 km, and future work will lead to an extension of this range. Currently, the deviation of temperatures from the radiosonde below 10 km is due to the presence of aerosols. The Mie scattering introduced by aerosols is preserved in N_{R-} but cut off in N_{L-}, so R_T decreases with stronger Mie scattering, leading to colder temperature if inferred from the aerosol-free calibration curves. For future improvement, we will form a third ratio from the signals in frequency f_a and use three-dimensional calibration curves to derive wind, temperature, and aerosol backscatter ratio in the lower atmosphere. The upper altitude is currently limited by photon noise to precisions of ±10 m/s and ±15 K. The low Na lidar power at 589 nm is a drawback of our technique. Nevertheless, the measurements can be extended to altitudes above 45 km with a larger telescope, better receiver design, and new lasers with higher power at 589 nm. The Nd:YAG-laser-based Rayleigh lidars have been capable of measuring wind with spectral analysis using Fabry–Perot or iodine filters or of measuring temperature with combined Raman and integration techniques; however, simultaneous wind and temperature capability has not yet been demonstrated for Rayleigh Doppler techniques. Owing to the combination of the multi-frequency transmitter and the double-edge magneto-optic filter, the simultaneous measurements of wind, temperature, and aerosol in a relatively large altitude range is a major advantage of Na-DEMOF technique over these systems.

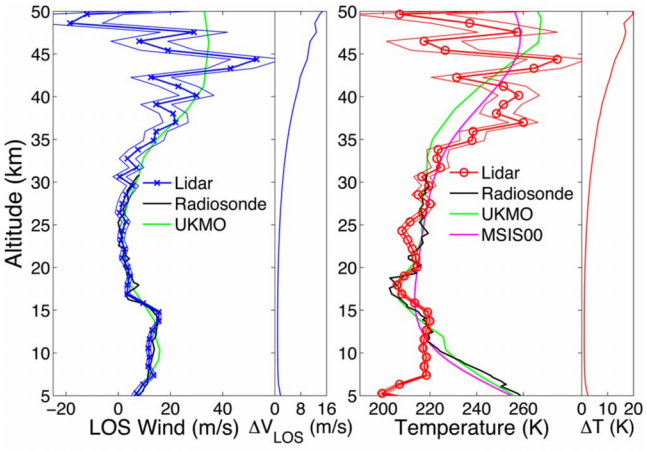

Fig. 4. (Color online) LOS wind (left) and temperature (right) measured on 9 January 2009 at Fort Collins, Colorado. Radiosonde and model winds are projected to LOS. $\Delta z = 1$ km and $\Delta t = 60$ min.

In conclusion, our field tests demonstrate the simultaneous profiling of wind and temperature with a Na-DEMOF implemented in the receiver of a three-frequency Na Doppler lidar. Under the current conditions of ~0.4 W lidar power and 75 cm telescope, reliable winds and temperatures are obtained from 10 to 45 km at resolutions of 1 km and 60 min, in agreement with radiosonde and model data. Such a multi-frequency edge-filter technique can be applied to other direct-detection Doppler lidars for profiling both temperature and wind. Combining with the wind and temperature measured by the resonance Doppler lidar in the MLT region, it is possible to profile wind and temperature simultaneously from the lower to the upper atmosphere. Such capability could lead to new scientific endeavors, including various dynamics studies. To achieve reliable lidar measurements independent of radiosonde calibration, the photodetectors must be calibrated in future work.

This research is supported by the CIRES Innovative Research Program, the National Science Foundation (NSF) ATM-0545353, ATM-0545262, and ATM-0545221, NSF CAREER ATM-0645584, and NSF ATM-0723229.

References

1. B. M. Gentry, H. Chen, and S. X. Li, Opt. Lett. **25**, 1231 (2000).
2. M. L. Chanin, A. Garnier, A. Hauchecorne, and J. Porteneuve, Geophys. Res. Lett. **16**, 1273 (1989).
3. J. S. Friedman, C. A. Tepley, P. A. Castleberg, and H. Roe, Opt. Lett. **22**, 1648 (1997).
4. J. W. Hair, L. M. Caldwell, D. A. Krueger, and C.-Y. She, Appl. Opt. **40**, 5280 (2001).
5. W. Huang, X. Chu, B. P. Williams, S. D. Harrell, J. Wiig, and C.-Y. She, Opt. Lett. **34**, 199 (2009).
6. X. Chu and G. C. Papen, in *Laser Remote Sensing*, T. Fujii and T. Fukuchi, eds. (CRC Press, 2005), pp. 179–432.